Available online at www.sciencedirect.com
SCIENCE DIRECT®
Journal of Chromatography A, 1060 (2004) 61–76
JOURNAL OF CHROMATOGRAPHY A
www.elsevier.com/locate/chroma

Synthesis and characterization of hypercrosslinked, surface-confined, ultra-stable silica-based stationary phases

Brian C. Trammell, Lianjia Ma, Hao Luo, Marc A. Hillmyer, Peter W. Carr*

Department of Chemistry, University of Minnesota, 207 Pleasant St. SE, Minneapolis, MN 55455, USA

Abstract

The synthesis and chromatographic characterization of a highly crosslinked self-assembled monolayer (SAM) stationary phase whose acid and thermal stability were significantly improved relative to a sterically protected octadecylsilane (ODS) stationary phase were recently described [B.C. Trammell, L. Ma, H. Luo, D. Jin, M.A. Hillmyer, P.W. Carr, Anal. Chem. 74 (2002) 4634]. Unfortunately, this highly crosslinked SAM phase is much more silanophilic than a conventional sterically protected octadecyl silane phase. ^{29}Si CP-MAS NMR analysis shows that the high concentration of silanol groups in the self-assembled monolayer causes the increased retention and poor peak shape of basic solutes. In this work dimethyl-chloromethyl-phenylethyl*chlorosilane* (DM-CMPES), a silane with only a single reactive silyl chloride group was tested as an alternative to chloromethyl-phenyethyl*trichlorosilane* (CMPES) as the basis for forming the starting phase. Most importantly this "conventional" silanization step (i.e., a non-SAM silanization) was followed by a Friedel-Crafts reaction using aluminum chloride as the catalyst and styrene heptamer as the multi-valent crosslinker to form the surface DM-CMPES groups into a network polymer which is fully confined and attached to the surface. An octyl (C_8) derivative of the hypercrosslinked (HC) dimethyl-chloromethyl-phenylethyl (DM-CMPES) surface-confined stationary phase was synthesized to demonstrate the potential of a Friedel-Crafts based approach to making high efficiency, acid and thermally stable polymerized phases on silica with selectivity closer to conventional aliphatic phases. The stability of the retention factors of these phases under very aggressive conditions (5%, (v/v) trifluoroacetic acid and 150 °C) are compared to that of a sterically protected octadecylsilane (ODS) phase. The comparisons show that the long term stability of highly crosslinked DM-CMPES phases in acid is superior to the conventional phase. The HC-C_8 phase is even more stable in acid than the HC-styrene heptamer DM-CMPES phase on which it is based. Additionally, the efficiency and peak shape of several prototypical bases under acidic (0.1% TFA, pH 2.0) elution conditions are discussed. The column dynamics and thermodynamic characteristics of the HC-C_8 phase were investigated to demonstrate the chromatographic utility of this ultra-stable phase. Inverse size exclusion chromatography and flow studies of the HC-C_8 and the sterically protected C_{18} stationary phases indicate the absence of pore plugging and quite good (nearly 100,000 plates/m) chromatographic efficiency. Further chromatographic investigations show that the HC-C_8 stationary phase behaves as a typical reversed phase material. The HC-C_8 stationary phase offers unique chromatographic selectivity for certain classes of analytes compared to both alkyl and phenyl bonded phases

Keywords: Stationary phases, LC; Dimethyl-chloromethyl-phenylethylchlorosilane; Self-assembled monolayer

1. Introduction

A great deal of work has gone into the development of acid (low pH) stable stationary phases for reversed phase liquid chromatography [2–19]. Acid stable phases are critically important for peptide and protein separations and for the liquid chromatographic–mass spectroscopic analysis of bases. Additionally, enhanced acid stability allows the chromatographer to more fully exploit selectivity differences and peak shape improvements for small, basic solutes under acidic mobile phase conditions. At this time the extraordinary stability of zirconia-based reversed phases in both acid and alkaline media has not led to improved separations of proteins and peptides due to irreversible adsorption of such analytes on zirconia surfaces [20,21].

Kirkland and coworkers [6,8,9] developed sterically protected phases which can be considered to be the current "gold

* Corresponding author. Tel.: +1 612 624 0253; fax: +1 612 626 7541.
E-mail address: carr@chem.umn.edu (P.W. Carr).

0021-9673/$ – see front matter © 2004 Elsevier B.V. All rights reserved.
doi:10.1016/j.chroma.2004.07.075

standard" for acid stable RPLC stationary phases. Two bulky isopropyl or isobutyl substituents on the silicon atom of the silane shield the underlying siloxane bond between the silane and the silica surface, thereby slowing acid-catalyzed hydrolysis and phase loss. Such sterically protected ODS phases show minimal losses in solute retention as measured by the decrease in k' of nonpolar solutes under highly aggressive mobile phase conditions (1.0%TFA, pH 1.0, 1.0 mL/min, 90 °C, 25,000 column volumes). However, these phases show nearly 50% loss in solute k' in only 1400 column volumes under accelerated acid aging conditions (5.0% TFA, pH 0.5, 2.0 mL/min, 150 °C) [1,22]. While we do not advocate the use of such harsh conditions for routine use, this accelerated aging test clearly illustrates that the sterically protected phases are not immune to acid catalyzed phase loss. It is also important to realize that because sterically protected phases are intended for use in acidic media they are not end-capped with small silanes that would, under acid conditions, be rapidly cleaved from the surface.

We believe it would be beneficial to improve the acid stability of RPLC phases beyond that provided by the sterically protected ODS phases. For example, certain classes of solutes (i.e., hydrophobic peptides and proteins) benefit significantly from higher mobile phase acidity and higher column temperatures. Further improvements in acid stability will also be necessary to enable high temperature ultra-fast liquid chromatography [23–26] especially for biomolecule separations. Additionally, longer column life under acidic mobile phase conditions reduces the amount of time and expense required to qualify new columns.

We have developed two types of highly crosslinked stationary phases that show dramatically better acid stability compared to sterically protected phases [1,22]. These highly crosslinked stationary phases are synthesized in two steps. First, a chlorinated aromatic silane is covalently bonded to the silica surface in either a surface assembled monolayer type process or by a conventional silanization. In a second step a Friedel-Crafts reaction catalyst is used to self-condense adjacent phenyl groups of the silanes to each other and to non-adjacent chloromethylphenyl groups by means of an added non-polymerizable multi-valent reagent (such as styrene heptamer). It is also possible to use additional Friedel-Crafts reaction steps to further crosslink or add desirable alkyl functional groups (e.g., octyl) to the hypercrosslinked, surface confined polymer.

There are several reasons for using covalently bonded chlorinated, aromatic silanes, aromatic crosslinkers and Friedel-Crafts chemistry to synthesize highly crosslinked stationary phases. First, covalent bonding of the reactive alkylchloro group completely confines the crosslinking process to the silica surface, thereby precluding any pore blockage. The use of a surface reagent, that reacts "orthogonally" with a multi-valent crosslinker, and cannot react with itself, is essential in this regard. Such reaction chemistry prevents formation of bulk polymer which can potentially plug pores and impede mass transfer in the stationary phase as it does in conventional polymer coating approaches [27–29]. The use of free radical and related non-orthogonal reactive moieties is largely self-defeating. Second, it is a property of the Friedel-Crafts chemistry that each time an alkyl crosslink is formed between two aromatic rings, the rings become more activated towards additional Friedel-Crafts reaction. Third, the aromatic network formed by crosslinking can be subsequently chloromethylated and re-crosslinked to further increase stability. Finally, the highly crosslinked aromatic network is easily derivatized by a wide variety of chemistries, thus leading to stationary phases with different chromatographic selectivities. We note that Davankov has made extensive use of Friedel-Crafts chemistry to make hyper-crosslinked polystyrene beads for ion exchange chromatography [30–32].

We have studied two types of highly crosslinked stationary phases. The first type uses a self-assembled monolayer (SAM) of chloromethyl-phenylethyl-trichlorosilane on silica as the starting phase. The SAM approach is very attractive because it provides a very high surface density of reactive chlorine for subsequent Friedel-Crafts crosslinking; however, the inevitable defects [17–19,33] in the monolayer produce many highly deleterious silanol groups. Details of its synthesis, and excellent acid and thermal stability were discussed in a recent publication [1]. A second type of highly crosslinked stationary phase, more recently communicated [22] and further elaborated here, uses a monomeric silane, dimethyl-chloromethyl-phenylethylchlorosilane (DM-CMPES), to bond the reactive chlorine to the silica. This type of "conventional" monomeric silanization (i.e., non-SAM) is much easier to perform than self-assembly and in contrast to the SAM process it cannot introduce additional silanols to the surface; however, the surface density of reactive chlorine is substantially lower than that of the material made by the SAM process, and thus it was not clear if a phase made from DM-CMPES as compared to one made from CMPES would be stable after Friedel-Crafts crosslinking.

2. Experimental

2.1. Chemicals and substrates

All solvents used in this work were HPLC grade. Acetonitrile was obtained from Burdick and Jackson (Muskegon, MI). Dichloromethane was obtained from Mallinkrodt-Baker (Paris, KY). Tetrahydrofuran was obtained from EM Science (Gibbstown, NJ). Acetone and isopropanol were obtained from PharmCo (Brookfield, CT). Trifluoroacetic acid (TFA) was from Spectrum (New Brunswick, NJ). Nitrobenzene, 1.0 M aluminum chloride in nitrobenzene, styrene heptamer (M_n = 770), and triphenylmethane were obtained from Aldrich (Milwaukee, WI). Chloromethyl-phenylethyl-dimethylchlorosilane (DM-CMPES) was obtained from Gelest Inc. (Tullytown, PA). The aluminum chloride in nitrobenzene solution and the DM-CMPES were stored under

nitrogen at all times. HPLC water was prepared by purifying house deionized water with a Barnstead Nanopure II deionizing system with an organic-free cartridge and a 0.2 μm final filter.

All chromatographic solutes were obtained from Aldrich (Milwaukee, WI) or Sigma (St. Louis, MO). Chromatographic solutes were dissolved in acetonitrile/water or pure THF (polystyrene standards) at a concentration of approximately 0.5–2 mg/mL.

Type B silica particles (Zorbax) from Agilent Technologies (Wilmington, DE) were used for all stationary phases. The particle diameter, surface area, pore diameter and pore volume of the particles are 4.8 μm, 180 m^2/g (BET), 80 Å and 0.4 mL/g, respectively.

2.2. Stationary phase synthesis

2.2.1. Highly crosslinked self-assembled monolayer stationary phases

The procedures for synthesizing the CMPES-SAM and for performing the Friedel-Crafts crosslinking were described in detail in a previous publication [1].

2.2.2. Monomeric silanization

The DM-CMPES silica was prepared by a slight modification of a method developed by Dorsey [34]. All glassware was rigorously cleaned in an ethanol–potassium hydroxide bath, rinsed thoroughly with HPLC water and dried at 150 °C overnight prior to use. Five grams of the Type B (100 Å pore diameter Zorbax) silica were dried under vacuum at 160 °C overnight prior to use. After cooling to room temperature under vacuum, the dried silica was slurried in a 250 mL round bottom flask using 100 mL of fresh dichloromethane (<0.01% water). The slurry was sonicated under vacuum for 30 min to fully wet the pores. After sonication, 32 μmol of 2,6-lutidine/m^2 of silica was added to the slurry. This amine acted as an "acid scavenger" and/or silanization catalyst. To the magnetically stirred slurry, 16 μmol of DM-CMPES/m^2 of silica were added. An activated alumina column inserted in the flask was used to prevent water access. The reaction mixture was refluxed at 50 °C for 24 h.

After 24 h, the silica particles were washed on a fritted glass funnel sequentially with 500 mL aliquots of dichloromethane, tetrahydrofuran, methanol, methanol/water, and acetone. After washing, the silica was dried under vacuum at 60 °C for a minimum of 4 h.

2.2.3. Friedel-Crafts crosslinking of the monomeric phase and derivatization

All glassware was cleaned and dried as described above. Three sequential Friedel-Crafts reactions were used to synthesize the *hypercrosslinked* C_8 phase. Each reaction was performed in a 150 mL roundbottom flask using 50 mL of nitrobenzene at 50 °C and a 5:1 molar ratio of $AlCl_3$:initial surface chloromethyl groups. The slurry was sonicated under vacuum at each step for 30 min to fully wet the particle pores. An appropriate amount of the $AlCl_3$ in nitrobenzene solution was transferred from the drybox and added to the slurry. An activated alumina column was used to prevent atmospheric water from deactivating the catalyst.

After each Friedel-Crafts synthesis step, the particles were filtered and washed sequentially on a medium porosity glass fritted funnel with 250 mL of fresh nitrobenzene, 500 mL of tetrahydrofuran, 30/70 tetrahydrofuran/water, and acetone. At the end of the reaction sequence, the stationary phase was dried under vacuum for 30 min at ambient temperature.

The first step in the reaction sequence was crosslinking with styrene heptamer and simultaneous self-condensation of the surface chloro methyl phenyl groups. The styrene heptamer:initial surface chloromethyl groups molar ratio was 2:1 (14:1 phenyl rings in the styrene heptamer:surface chloromethyl groups). It is very important to note that the reaction chemistry between the surface and the multi-valent crosslinking reagent is "orthogonal", that is, the crosslinking agent (styrene heptamer) cannot react with itself to form bulk polymer which could then plug pores or become attached to the surface. In this regard the approach to forming a highly interconnected polymer on the surface used here is unique. The second reaction used methoxychloromethane to further crosslink the stationary phase and provide chloromethyl groups for the third reaction. The CH_3OCH_2Cl:initial surface chloromethyl group molar ratio was 10:1. In a third reaction, 1-phenyloctane groups were added to the residual chloromethyl groups from the second reaction. After 24 h, a large molar excess of benzene was added to the reaction mixture to "endcap" any remaining chloromethyl groups. This step was deemed important in that alkyl chloro groups could well hydrolyze during use or react with analytes or mobile phase components which are strong electrophiles.

The stationary phases synthesized here were washed in situ in a packed column using an ACN/water/TFA gradient to remove residual Al^{3+} from the Friedel-Crafts crosslinking steps prior to characterization. Mobile phase A was 7.5/87.5/5.0 ACN/water/TFA (v/v/v) and mobile phase B was 87.5/7.5/5.0 ACN/water/TFA (v/v/v). The gradient profile was as follows: 0–5 min = 100% A, 5–20 min = 100% A to 100% B, 20–25 min = 100% B. The gradient was run at a flow rate of 2.0 mL/min and a column temperature of 150 °C. Four gradient cycles were used to attempt to completely remove all Al^{3+} deposited during synthesis. It is important to note that only in the case of the stability testing were the stationary phases not washed in an acidic eluent. All other chromatographic testing was done on columns subjected to the hot acidic gradients described above.

2.3. Elemental analysis

Carbon, hydrogen, and chlorine analyses were performed by Atlantic Microlabs, Norcross, GA, and MicroAnalysis Inc., Wilmington, DE.

2.4. ^{29}Si and ^{13}C CP-MAS NMR analyses

^{29}Si and ^{13}C CP-MAS NMR spectra were obtained on a Chemagnetics CMX-400 spectrometer operating at 100.45 and 79.80 MHz, respectively. All samples were spun at 5–6 kHz. Typically, spectra were obtained by using a contact time of 5 ms and a pulse repetition time of 1–2 s. A 90° pulse width of 6 μs was used for both ^{29}Si and ^{13}C experiments, which corresponds to a spin-lock field of 42 kHz. For ^{13}C CP experiments, the Hartmann-Hahn match was established using a sample of hexamethylbenzene (HMB), and the chemical shifts were referenced to 17.4 ppm for the methyl resonance of HMB. The single pulse ^{13}C spectra were obtained on the same spectrometer with a 90° pulse width of 6 μs and pulse delay of 1 s. For ^{29}Si CP experiments, a sample of 2,2-dimethyl-2-silapentane-5-sulfonic acid, which resonates at 0 ppm, was used to establish the Hartmann-Hahn condition.

2.5. DRIFT analysis

Each sample was prepared by combining 0.9 g of IR grade potassium bromide with 0.1 g of a silica-based stationary phase. The mixtures were ground in a mortar and pestle for 5 min. Each was then dried under vacuum at 160 °C overnight to remove adsorbed water. After heating, the samples were allowed to cool to room temperature under vacuum.

DRIFT spectra were collected on a Nicollet FT-IR spectrometer using the DRIFT optical stage. The sample compartment was under N_2 purge at all times. The MCT detector was cooled with liquid nitrogen for a minimum of 15 min prior to the collection of the IR grade potassium bromide background. Each spectrum was collected using 256 scans with a resolution of 4 cm^{-1}.

2.6. Chromatography columns

All stationary phases were packed in 5.0 cm × 0.46 cm columns. Stainless steel column hardware was obtained from Isolation Technologies (Hopedale, MA). The approximately 0.8 g of each phase was slurried in 8 mL of isopropanol and sonicated for 20 min prior to packing. Columns were packed by downward slurry technique at a packing pressure of 5000 psi (345 bar) using pure isopropanol as the driving solvent.

2.7. Chromatography experiments

Chromatographic experiments were performed on an HP 1090 Series II chromatograph. For the acid stability tests, a heating apparatus from Systec Inc. (New Brighton, MN) was used to control the column temperature. This apparatus consists of a mobile phase preheater assembly and insulating jacket, which allows the column to be heated to 200 °C. Unless otherwise noted all data were obtained using 1.0 μL injection volumes of solute with an absorbance detector set to a wavelength of 254 nm.

Dynamic acid stability testing was performed using a 47.5/47.5/5.0 by volume ACN/water/TFA (the pH of the water/TFA is 0.5) mobile phase at a flow rate of 2.0 mL/min and a column temperature of 150 °C. A 50/50 by volume ACN/water mobile phase was flowed through the column at 2.0 mL/min and 150 °C for 15 min prior to testing to allow the column to reach the set temperature. The eluent was then switched to that containing acid for aggressive aging. The mobile phases flow rates and column temperatures used for the chromatographic studies are given in the figure captions.

Silanophilicity characterization was performed by separating basic solutes in ACN/water mixtures contained TFA. Inverse size exclusion chromatography was performed with toluene and low polydispersity polystryrene standards (M_w = 1000–18,700 g/mol) in pure THF mobile phase at a flow rate of 1.0 mL/min and a column temperature of 40 °C using UV detection at 254 nm. The diameter of the polystyrene probes was calculated using the method of Halasz and Martin [35,36]. Flow curve analysis was performed over a reduced velocity range of approximately one to twenty using alkylphenones (k' = 2–25) as the probe solutes. Diffusion coefficients were taken from Li and Carr [37].

3. Results and discussion

3.1. Characterization of the silanophilicity of the highly crosslinked styrene heptamer CMPES-SAM

Fig. 1 shows the separation of several basic drugs at pH 1.0 on a sterically protected ODS stationary phase. With the exception of meclizine, the peaks are reasonably symmetric with acceptable plate counts. This chromatogram is our benchmark for silanophilicity. The sterically protected C_{18} was chosen for two reasons. First, like the highly crosslinked styrene heptamer stationary phases described here, the sterically protected C_{18} phase is not endcapped and is designed for use in at low pH. Second, the highly crosslinked phases were synthesized on the same Zorbax Type B silica particles as the commercial sterically protected C_{18} material, thus eliminating any differences in silanophilicity that might have been attributed to differences in the underlying silica.

Fig. 2A shows the separation of selected basic drugs from Fig. 1 on the highly crosslinked styrene heptamer CMPES-SAM phase. The peak shape is extremely poor for all the drugs. The U.S.P. tailing factor for each drug is significantly worse (factor of 2–8) on the highly crosslinked styrene heptamer CMPES-SAM phase compared to the sterically protected C_{18}. Additionally, the retention factors for all the basic drugs are significantly higher on the highly crosslinked styrene heptamer CMPES-SAM phase compared to the ODS phase despite the use of a mobile phase with a higher elution strength. The substantially higher U.S.P. tailing factors and higher retention factors for the basic drugs clearly indicate

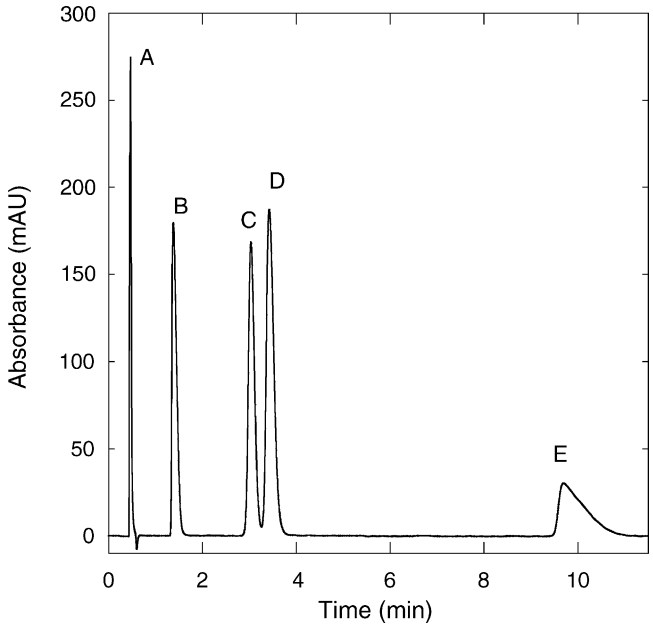

Fig. 1. The separation of bases on a sterically protected ODS phase. Solutes: (A) pyridine, (B) alprenolol, (C) nortriptyline, (D) amitriptyline, (E) meclizine. Mobile phase: 35/65 1.0% TFA in ACN/1.0% TFA in H_2O; pH 1.0; flow rate = 1 mL/min; temperature = 40 °C.

that the highly crosslinked styrene heptamer CMPES-SAM phase is much more silanophilic than the sterically protected ODS stationary phase. Fig. 2B further supports this conclusion. The addition of 50 mM *n*-hexylamine, a strong competitor for silanol sites, to the mobile phase both decreases retention and improves peak shape for all basic solutes. Many other silanol blocking agents were tested, but none produced peak shapes as good as those observed on the sterically protected ODS phase.

3.2. Spectroscopic and chromatographic examination of the CMPES-SAM phase

The high silanophilicity of the highly crosslinked styrene heptamer CMPES-SAM phases is chromatographically problematic. Its superior acid stability will not be generally useful if the phase gives poor peak shapes for basic solutes. We hypothesize that there are three possible causes for the high silanophilicity of the highly crosslinked styrene heptamer CMPES-SAM phase. First, there may be defects [33] in the self-assembled monolayer that provide a significant number of silanol sites many of which are strongly acidic. Second, the phase may be contaminated with Al(III) during the Friedel-Crafts crosslinking step. Metal contamination on the surface of the silica would increase the acidity of nearby silanols, thus leading to poorer peak shapes for basic analytes. Third, it is possible that both of the above hypotheses contribute to the high silanophilicity.

The most effective method for probing the quality of the CMPES-SAM is ^{29}Si magic angle spinning cross-polarization solid-state NMR spectroscopy. Wirth and coworkers [17,33,38] have shown that it is very powerful for characterizing SAM chromatographic materials. Four distinct resonances in the spectrum are particularly useful. The signals at −110 and −100 ppm correspond to the siloxane (SiO_4) and isolated silanols (SiO_3OH) of the silica substrate, respectively. Resonances at −70 and −59 ppm correspond to the completely bonded ($RSiO_3$) and isolated defect ($RSiO_2OH$) silicon atoms in the self-assembled monolayer, respectively. Based on molecular modeling, Wirth determined that a 100% methyl-SAM (produced by self-assembling methyltrichlorosilane on a *flat* silica surface) is essentially defect-free [18]. The situation for highly fractal, chromatographic silica is quite different. Wirth showed that a 100% methyl-SAM on chromatographic silica is not defect-free. This result clearly indicates the importance of the silica's

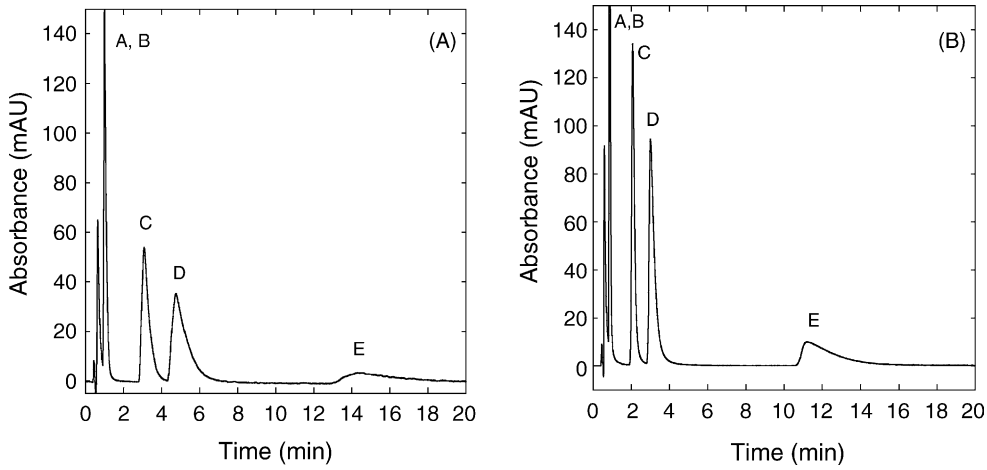

Fig. 2. Separation of bases on styrene heptamer crosslinked CMPES-SAM. (A) 45/55 1.0% TFA in ACN/1.0% TFA in H_2O, pH 1.0. (B) 45/551.0% TFA in ACN/1.0% TFA in H_2O, 50 mM *n*-hexylamine. Solutes and other conditions are as in Fig. 1.

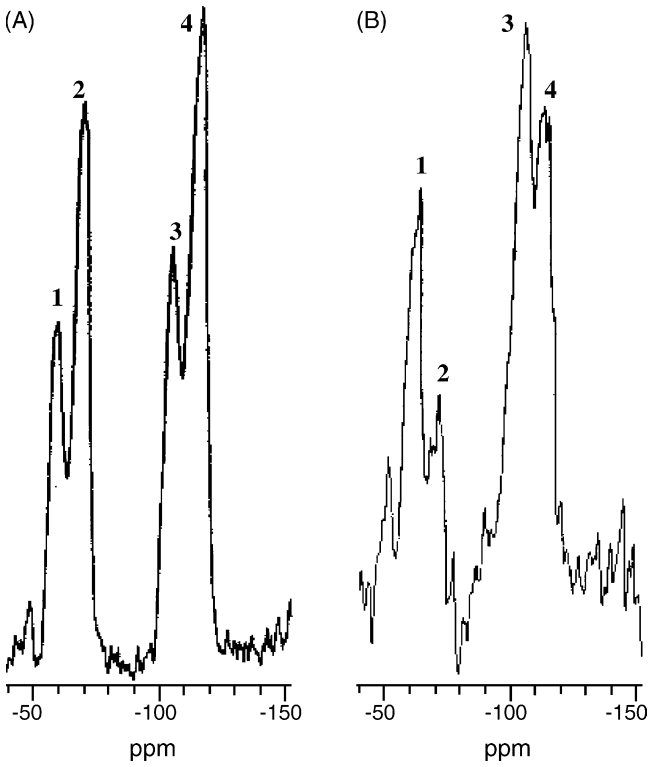

Fig. 3. ^{29}Si CP-MAS NMR spectra of self-assembled monolayer stationary phases. (A) 100% Methyl-SAM. (B) 100% CMPES-SAM. (1) $RSiO_3$-OH (−59 ppm); (2) $RSiO_3$ (−70 ppm); (3) SiO_3-OH (−100 ppm); (4) SiO_4 (−110 ppm).

surface geometry on the quality of the resulting SAM. However, it is reasonable to use the NMR spectrum of the 100% methyl-SAM as a benchmark for a "low-defect" SAM.

In order to compare the CMPES-SAM phase to a "low-defect" SAM, a 100% methyl-SAM was prepared and characterized by ^{29}Si CP-MAS NMR spectroscopy. The spectra for the 100% methyl-SAM and the CMPES-SAM phases are shown in Fig. 3A and B, respectively. The NMR spectra for these phases are rather different. The CMPES-SAM has significantly more isolated silanol defects than the 100% methyl-SAM. Additionally, the ratio of the peak heights for the silica isolated silanol (SiO_3OH) resonance and the silica siloxane (SiO_4) resonance peak heights are significantly higher for the CMPES-SAM compared to the 100% methyl-SAM. This shows that the CMPES-SAM is not as extensively bonded to the silica surface, as is the 100% methyl-SAM. Overall, the CMPES-SAM phase has a substantially higher population of silanols compared to the 100% methyl-SAM. Based on this NMR data, we concluded that defects in the CMPES-SAM are at least partly to blame for the poor peak shape of the basic drugs.

The high silanophilicity of the CMPES-SAM phase is further illustrated by comparing the U.S.P. tailing factors for three basic solutes on three different phases (see Fig. 4). The sterically protected C_{18} phase gives the lowest tailing factors. More importantly, the non-crosslinked CMPES-SAM (which had *never* been exposed to $AlCl_3$) gives the highest U.S.P.

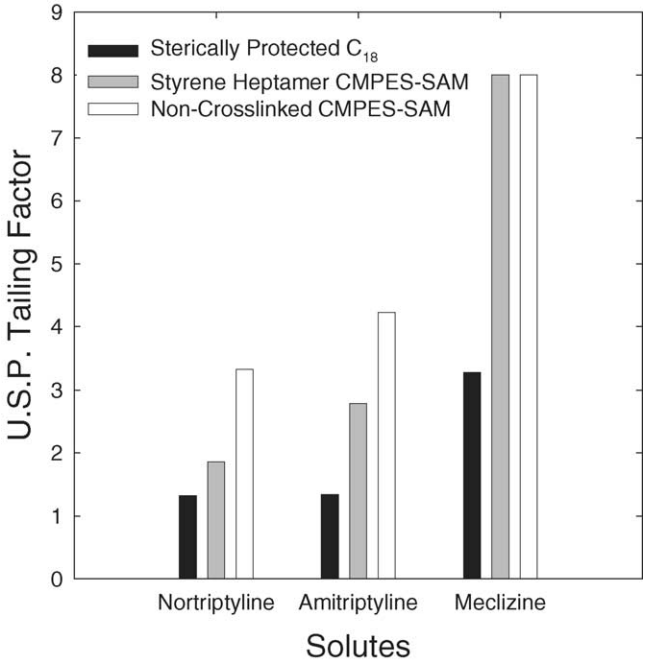

Fig. 4. U.S.P. tailing factor and results for selected bases at pH 1.0. Mobile phase: as in Fig. 1 for the sterically protected ODS phase, as in Fig. 2A for the CMPES phases.

tailing factor (i.e., worst peak shape) for all of the solutes. The styrene heptamer crosslinking step actually improves the peak shape for nortriptyline and amitriptyline. The reason for this is unknown. It is possible that the highly crosslinked styrene heptamer blocks access to a proportion of the silanols in the CMPES-SAM and on the silica surface, thus leading to improved peak shape. Based on these observations along with the above NMR data we conclude that the CMPES-SAM itself is extremely silanophilic towards organic cations and therefore, it is not a viable route to making highly crosslinked stationary phases with low silanophilicity. It has been suggested that if the initial SAM layer of CMPES were synthesized using an appropriate ratio of trichloromethyl silane and chloromethyl-phenylethyl-trichlorosilane the surface concentration of free silanol groups could be decreased greatly [39]. This must be tested in the future.

3.3. Synthesis and elemental analysis of highly crosslinked styrene heptamer monomeric stationary phases

In order to overcome the poor chromatographic performance of the basic drugs on the highly crosslinked styrene heptamer CMPES-SAM stationary phase, we developed and tested a highly crosslinked *monomeric* phases. Specifically, DM-CMPES was covalently bonded to silica. Both the carbon and chlorine content data show that a reasonably high surface density of DM-CMPES groups (approximately 2.9 μmol/m^2) was achieved. This is, in itself, significant in that we could not use maximally active aliphatic amine catalysts in the

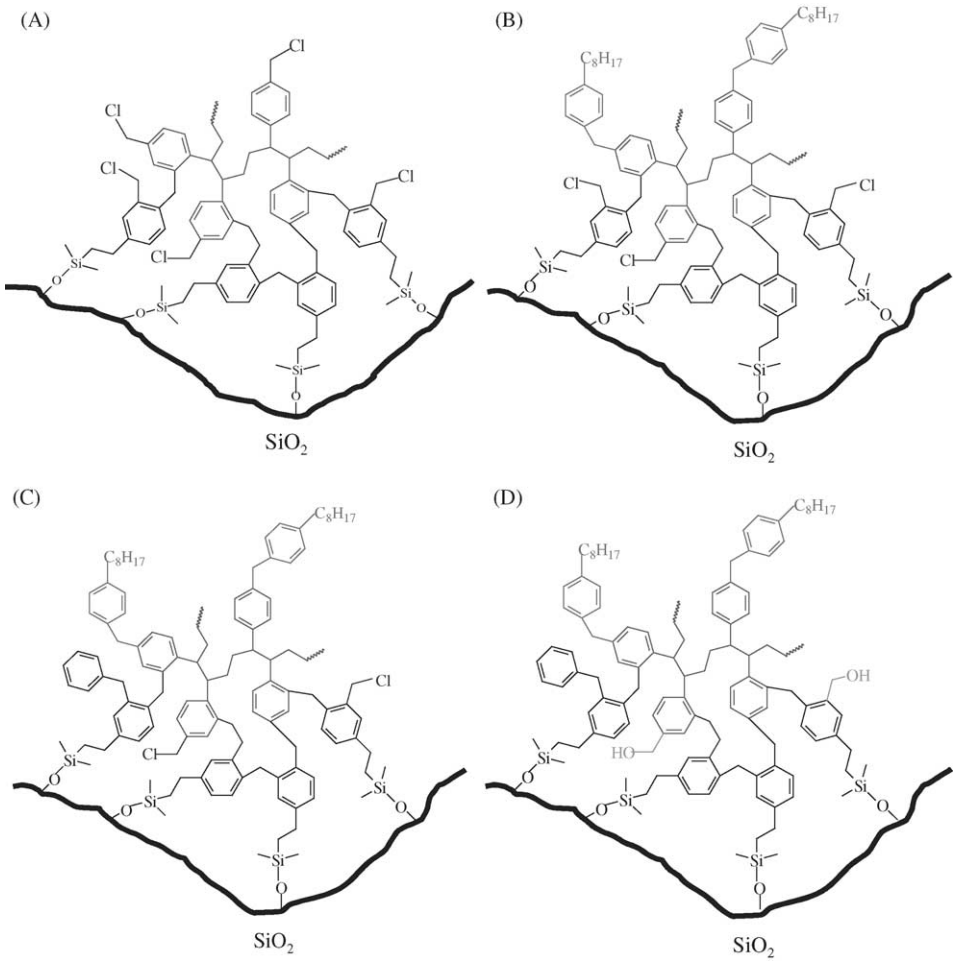

Fig. 5. Representation of the synthesis steps for making the HC-C_8 stationary phase. (A) Chloromethylation and secondary crosslinking of HC-styrene heptamer DM-CMPES. (B) Derivatization with octylbenzene. (C) Removal of chlorine by reaction with benzene or "endcapping". (D) Removal of residual chlorine by hydrolysis.

silanization process as they react with the chloromethyl group of DM-CMPES. The best commercially available dimethyl alkyl silane stationary phases have at most 3.0–3.5 μmol/m^2 of bonded ligands [14,40,41]. The silanization step was followed by Friedel-Crafts chemistry to obtain a highly crosslinked styrene heptamer DM-CMPES stationary phase. This phase was then used as the starting material for a hyper-crosslinked, surface-confined octylbenzene derivative phase. A schematic representation of the HC-C_8 phase is shown in Fig. 5. There are three Friedel-Crafts steps in the synthesis of this phase after the initial silanization with DM-CMPES and Friedel-Crafts crosslinking with styrene heptamer. The steps are chloromethylation and secondary crosslinking, octylbenzene derivatization, and benzene "endcapping".

In order to better understand this multi-step synthesis, the product from each stage in the reaction was characterized by elemental analysis. The elemental analysis data are summarized in Table 1. Based upon the carbon and chlorine content, the chloromethylation and secondary crosslinking step adds 5.60 ± 0.05 μmol/m^2 of CH_2 crosslinks and 3.3

Table 1
Summary of elemental analysis[a] data at each stage in the synthesis of the HC-C_8 stationary phase

Reaction	Percent carbon (±0.10%)	Percent hydrogen (±0.10%)	Percent chlorine (±0.2%)
Stable bond C_{18}	10.10	Not measured	0.00
Chloromethylation—secondary crosslinking	8.84	0.65	2.10
Phenyl-C_8 derivatization	12.76	0.93	0.86
Benzene endcapping	13.20	1.34	0.50
After stability testing[b]	13.00	1.36	0.00

[a] w/w_{SiO_2}.
[b] The material was unpacked from the column after the stability test shown in Fig. 3 was conducted.

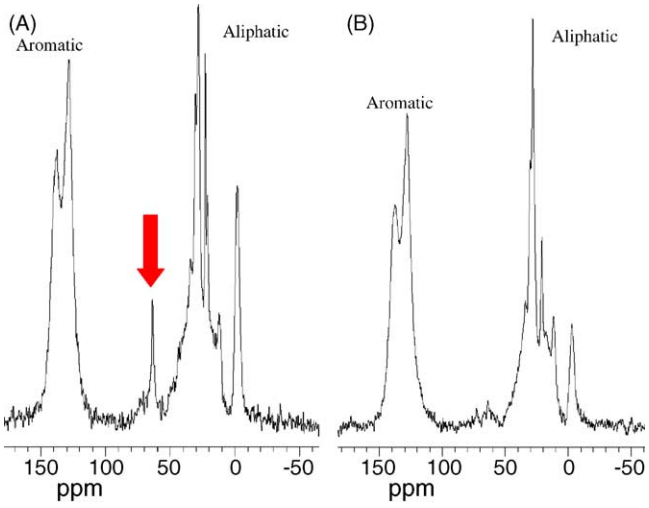

Fig. 6. ^{13}C NMR characterization of HC-C_8 before (A) and after (B) acid washing. The resonance under the arrow corresponds to the CH_2Cl group.

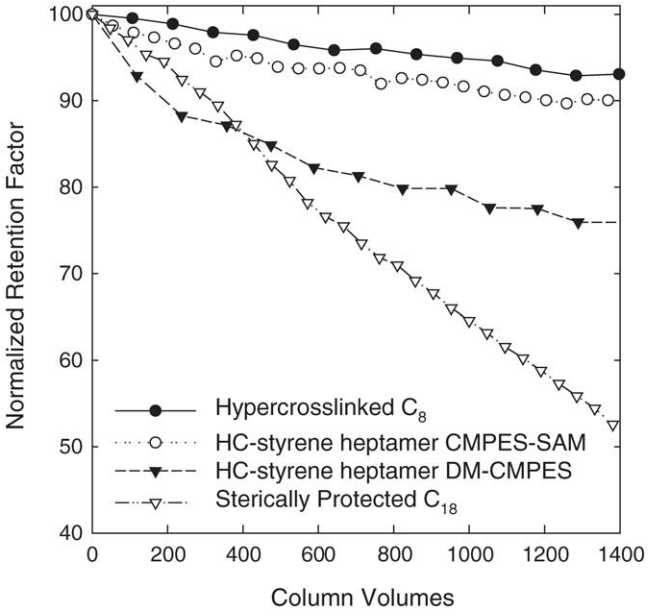

Fig. 7. Dynamic acid stability of the hypercrosslinked and the sterically protected C_{18} stationary phases. Mobile phase: 47.5/47.5/5.0 ACN/H_2O/TFA, pH 0.5; T = 150 °C; flow rate = 2.0 mL/min; solute = dodecanophenone; all columns were 5.0 cm × 0.46 cm.

± 0.1 μmol/m^2 of chloromethyl groups. The percent carbon increase indicates that octylbenzene derivatization results in the bonding of 1.30 ± 0.05 μmol/m^2 of octylbenzene chains to the hypercrosslinked stationary phase. The decrease in chlorine content after octylbenzene derivatization is 1.2% (w/w). This corresponds to 1.9 ± 0.1 μmol/m^2 of chlorine consumption. The decrease in the surface density of chlorine is greater than is the increase in surface density of octylbenzene groups added to the phase. This suggests that some octylbenzene groups are multiply bonded to the hypercrosslinked phase. The chlorine content after octylbenzene derivatization is 0.86% (w/w) or 1.4 ± 0.1 μmol/m^2. Benzene "endcapping" adds 0.34 ± 0.05 μmol/m^2 of benzene. Once again, the amount of chlorine consumed (0.6 ± 0.1 μmol/m^2) in the reaction exceeds the amount of benzene added, also suggesting the formation of multiple bonds between the added benzene rings and the stationary phase surface. Both the elemental analysis data, and ^{13}C NMR spectra before and after acid hydrolysis shown in Fig. 6 indicate that the residual 0.8 ± 0.1 μmol/m^2 of chloromethyl groups are completely hydrolyzed to –CH_2OH groups upon treatment with the four, hot acid gradient elution runs. Note that the resonance of the CH_2OH group is hidden under other peaks.

3.4. Acid stability of HC-styrene heptamer DM-CMPES and HC-C_8

The dynamic acid stability comparison of the HC-styrene heptamer DM-CMPES, HC-C_8 and the sterically protected C_{18} stationary phases are shown in Fig. 7. The retention stability curve for the silanophilic HC-styrene heptamer CMPES-SAM phase is included for comparison. The HC-C_8 phase is the most stable phase under these very aggressive test conditions. This indicates that a self-assembled monolayer is not a prerequisite for the preparation of an ultra stable phases for low pH applications. The retention stability curves also indicated that the HC-C_8 phase is much more stable than either of the other monomeric phases under these very aggressive acid aging conditions. The significant improvement in acid stability for the HC-C_8 phase compared to its parent phase, the HC-styrene heptamer DM-CMPES phase, illustrates the significant benefit of the second crosslinking step and the addition of the alkyl groups. The HC-C_8 phase loses only 7% of its initial retention compared to the approximately 22% loss in retention experienced by its parent phase. Note that neither material was "pre-stressed" or "pre-treated" with strongly acidic media prior to stability testing (see Section 2). The sterically protected C_{18} phase is the least stable phase showing a loss of nearly 50% of its initial retention in 1400 column volumes.

Elemental analysis for carbon on the HC-C_8 material prior to and after stability testing (see Table 1 last two rows) indicates a decrease in carbon content from 13.2% to 13.0%. This is a much smaller change than the 22% decrease in k'. We believe that the much larger decrease in k' comes about not due to a commensurate loss in carbon content but is primarily due to changes in the polarity of the stationary phase by two processes: first and possibly of lesser importance is the hydrolysis of CH_2Cl groups to CH_2OH groups (note the change in %Cl in Table 1) and second by hydrolysis of the vast majority of the siloxane bonds which hold the polymerized network on the surface. ^{29}Si NMR spectroscopy (data not shown) indicates that a very large increase in silanol population occurs after the hot acid treatment. We also point out that our previously published SEM results show the extreme stability of the polymer layer even after all the underlying silica is removed by dissolving it in hydrofluoric acid [22].

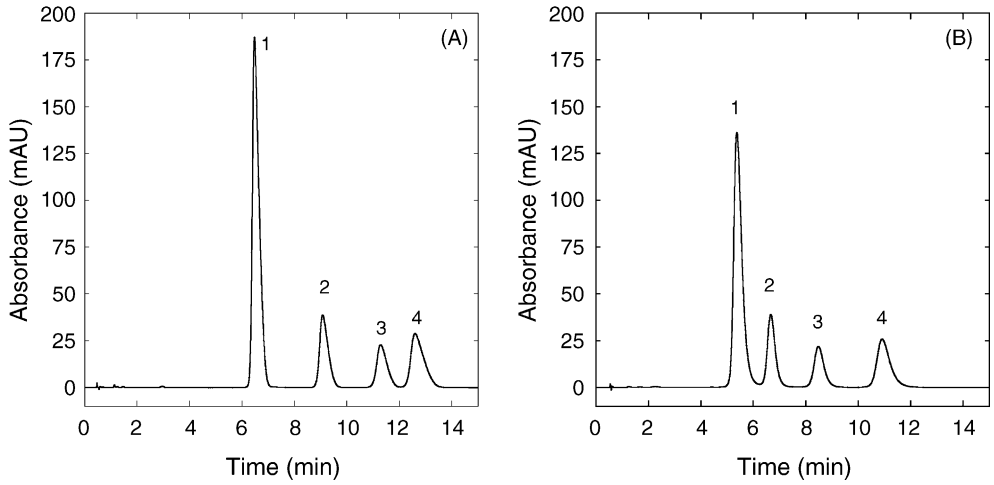

Fig. 8. Separation of basic drugs. (A) Sterically protected C_{18}; 22/78 0.1% TFA in ACN/0.1% TFA in H_2O, pH 2.0. (B) HC-C_8; 15/85 0.1% TFA in ACN/0.1% TFA in H_2O, pH 2.0. Solutes: (1) perphenazine, (2) desipramine, (3) nortriptyline, (4) amitriptyline; temperature = 35 °C; flow rate = 1.0 mL/min.

3.5. *Silanophilicity of the highly crosslinked C_8 monomeric stationary phases*

As discussed in the Section 2, the column was pre-treated with an acidic mobile phase prior to peak shape evaluation in order to remove residual Al^{3+} from the Friedel-Crafts catalyst. As stated above, substantial enhancements in acid stability are important; however, the enhancement cannot be procured at the price of significantly diminished peak shape quality. The separations of several prototypical basic solutes at pH 2.0 on the sterically protected C_{18} and the HC-C_8 stationary phases are shown in Fig. 8. The volume fraction of acetonitrile in the mobile phase was decreased by 7% (v/v) on the HC-C_8 phases to obtain similar retention factors, thus allowing for a more even handed comparison of the basic drug peak shapes. Visually, both phases give similar peak shapes for the basic drugs. A more quantitative comparison of the retentivity, efficiency and peak shape offered by the sterically protected C_{18} and the HC-C_8 phases is shown in Fig. 9.

It is clear from Fig. 9A that the HC-C_8 phase is less retentive that the sterically protected C_{18} for both non-electrolyte and basic solutes despite using a lower elution strength mobile phase. This finding is not entirely surprising given the low density of C_8 chains (1.4 μmol/m^2) on the phase. Fig. 9B shows that the plate counts for non-electrolyte solutes are very similar on both phases (N = 90,000–100,000/m); however, the plate counts for basic solutes are definitely lower on the HC-C_8 phase. This is most likely due to hydrolysis of siloxane bonds between the highly crosslinked phase and the silica surface during the acidic cleaning step required to remove residual Al^{3+} (see Section 2). Alternative, less destructive cleaning methods are currently under investigation. The U.S.P. tailing factors for the solutes are shown in Fig. 9C. The U.S.P. tailing factor is defined as:

$$T_f = \frac{a+b}{2a} \quad (1)$$

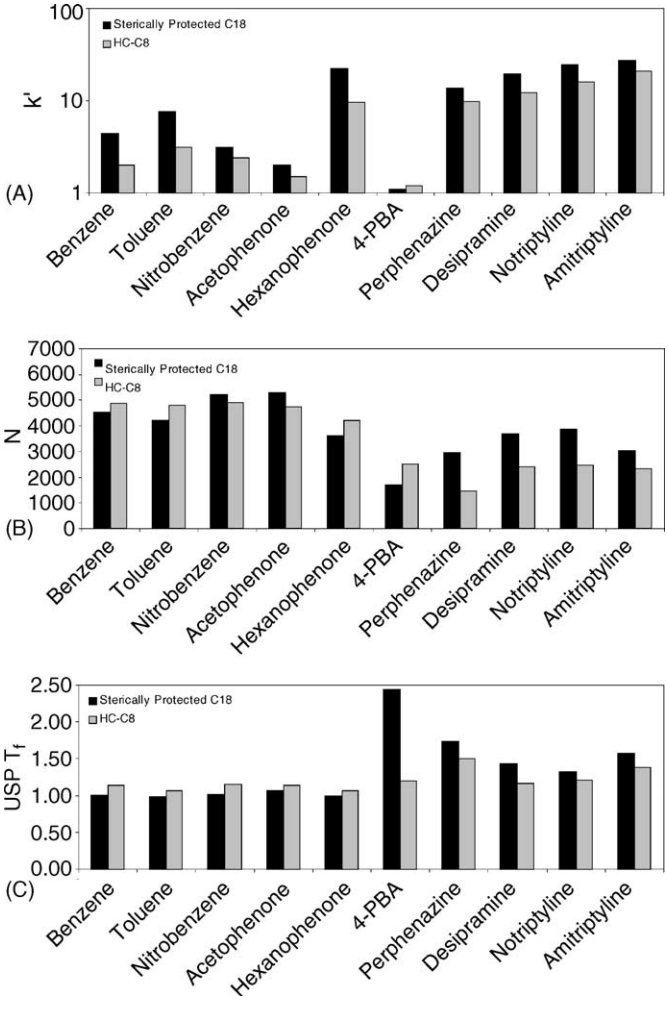

Fig. 9. The comparison of retention factor, plate count and U.S.P. tailing factor of select solutes on the sterically protected C_{18} and the HC-C_8 phases. Flow rate: 1.0 mL/min; temperature = 35 °C; non-electrolyte solutes: 45/55 ACN/water, 4-phenyl butyl amine: 28/72, 0.1% TFA in ACN/, 0.1% TFA in water, pH 2 (sterically protected C_{18}), 10/90 0.1% TFA in ACN/, 0.1% TFA in water, pH 2 (HC-C_8); basic solutes: same mobile phases as in Fig. 8.

where *a* is the front half-width of the peak at 5% peak height and *b* is the back half-width of the peak at 5% peak height. The U.S.P. tailing factors for all of the basic solutes are closer to unity (less tailed) on the HC-C_8 phase compared to the sterically protected C_{18}. The lower tailing factors of the HC-C_8 phase help explain why the solute peak shapes look quite similar in Fig. 8 despite the higher plate counts of the sterically protected C_{18} phase. The difference in U.S.P. tailing factors is especially evident for 4-phenylbutylamine (4-PBA). The U.S.P. tailing factor for 4-PBA is 2.4 on the sterically protected C_{18}, but only 1.2 on the HC-C_8 phase. Although the same amount of sample was injected on both phases, column overloading on the sterically protected C_{18} phase may be the cause of the overall higher U.S.P. tailing factors. McCalley [42] has studied the effect of overloading RPLC columns with basic analytes on the evaluation of efficiency and tailing. Preliminary results (not given here) suggest that the sterically protected C_{18} phase tends to "overload" more easily than the HC-C_8 phase, thus helping to explain the higher tailing factor for 4-PBA on the sterically protected C_{18} phase. A detailed study of the silanophilicity of HC-C_8 is currently underway.

In additional to possible differences in the basic solute mass loadability of the phases, the lower U.S.P. tailing factors on the HC-C_8 phase is conceivably due to the presence of CH_2OH groups in the stationary phase that are acting as polar embedded groups. These hydroxyl groups result from conversion of CH_2Cl groups to CH_2OH groups. It is possible that the CH_2OH groups provide additional shielding of the silanol groups via hydrogen bonding, thus leading to lower U.S.P. tailing factors. Within the last few years, several stationary phase manufacturers have developed "polar-embedded" phases which generally show additional silanol shielding resulting from hydrogen bonding interactions between a polar functionality (e.g., an embedded amide group) and the silanols on the surface. Polar embedded phases generally show improved peak shapes for basic drugs compared to a conventional alkyl bonded phase.

3.6. *Efficiency characterization of the HC-C_8*

The pore accessibility and chromatographic efficiency of the HC-C_8 stationary phase were evaluated by inverse size exclusion chromatography and van Deemter analysis of the flow curves. Related data for the sterically protected C_{18}, bare silica and the HC-C_8 phases are given below.

Inverse size exclusion chromatography allows a comparison of pore accessibility of different substrates through elution volume measurements of a series of polymeric samples of well-defined molecular weight [35,36,43–45]. The pore accessibility of the bare silica used in the synthesis of the crosslinked self-assembled monolayer phases was evaluated to determine how each step in the synthesis effects the pore volume. As shown in Fig. 10, the pore volume decreases as the total amount of stationary phase (as measured by carbon content) increases. The pore volume

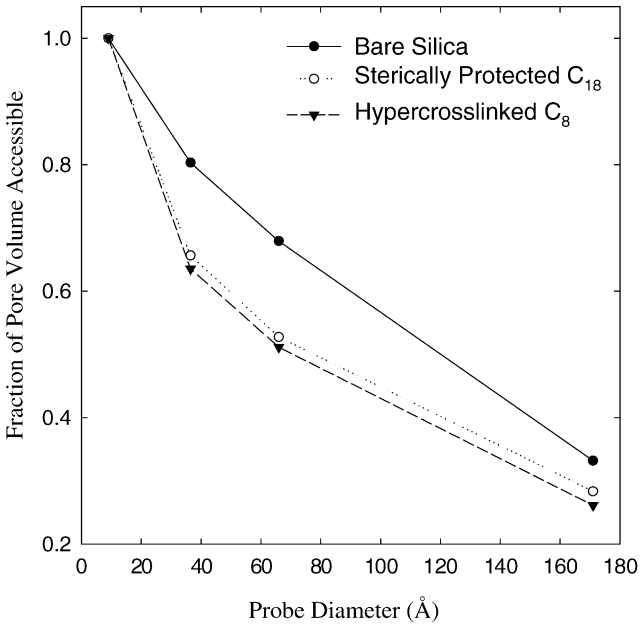

Fig. 10. Plot of pore accessibility of sterically protected C_{18} and HC-C_8 stationary phases by inverse size exclusion chromatography with polystyrene standards. Mobile phase: 100% THF; temperature = 40 °C; flow rate = 1.0 mL/min, UV detection at 254 nm.

of the HC-C_8 is the lowest of all phases, but this must be so because it has the highest carbon loading.

For chromatographic stationary phases, it is very important to determine whether or not the synthetic process results in significant pore blockage [28,46]. It is well known that pore blockage can lead to poor mass transfer in the stationary zone, thus giving poor chromatographic efficiency [47]. Some simple calculations [1] using the inverse size exclusion chromatography data shown in Fig. 10 and the carbon composition allow for a much more quantitative comparison of the stationary phases. We compare the change in pore volume as calculated from inverse size exclusion chromatography data with that based on the carbon content. If significant pore blocking is occurring, the $V_{PHASE,\,ISEC}$ will be larger than the calculated $V_{PHASE,\,\%C}$. For a reasonably uniform coating of stationary phase (little or no pore blockage), the $V_{PHASE,\,ISEC}$ will be approximately equal to the calculated $V_{PHASE,\,\%C}$ [27,46].

The results of this comparison are given in Table 2. The $V_{PHASE,\,ISEC}$ for the HC-C_8 is approximately equal to the calculated $V_{PHASE,\,\%C}$. This is good evidence that none of the steps in the stationary phase synthesis leads to pore blockage of the silica. [48,49] We believe that this confirms our hypothesis that the polymer formation by our orthogonal reaction route is confined to the surface. At this time we have not carried out nitrogen adsorption studies of the pore structure but prior work has led us to the conclusion that ISEC is chromatographically more relevant and provides more directly useful information.

The HC-C_8 and the sterically protected C_{18} stationary phases were further compared by generating a "flow curve"

Table 2
Calculated pore accessibility data for sterically protected C_{18} and the HC-C_8 stationary phase

Stationary phase	Percent carbon (±0.10%)	V_{PORE} by ISEC	Calculated V_{Phase} by %C[a] (mL/column)	Calculated V_{Phase} by ISEC (mL/column)
Bare silica	0.0	0.239	0.000	0.000 mL
Sterically protected C_{18}	10.1	0.176	0.107	Not available[b]
HC-C_8	13.0	0.176	0.065	0.061 mL

[a] A reasonable estimate for the density of the phases was used in the calculation (1.3 g/mL for the HC-C_8 phase, 0.80 g/mL for sterically protected C_{18}).
[b] The pore volume of the bare silica used for this stationary phase was not provided by the manufacturer.

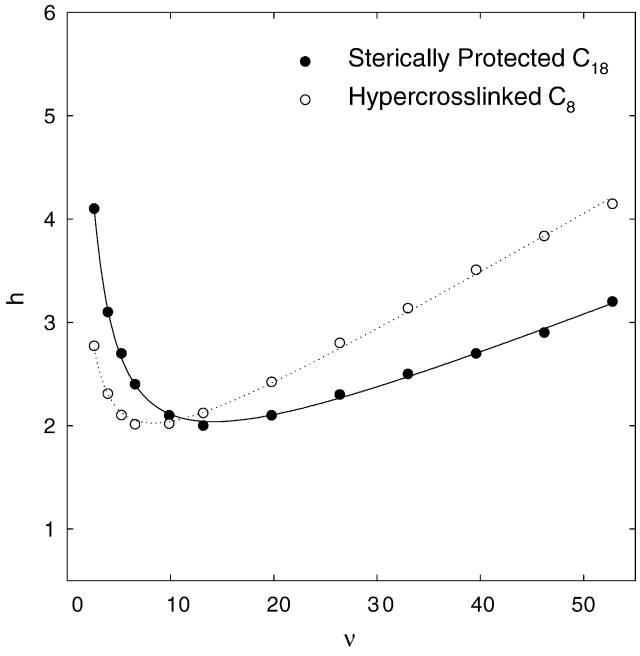

Fig. 11. Analysis of van Deemter curve of sterically protected C_{18} and HC-C_8. The van Deemter equation was used to obtain the curve fit. Solute: butanophenone; mobile phase: 30/70 ACN/H_2O; T = 40 °C, sterically protected C_{18}: k' = 24.5, h_{min} = 2.04; HC-C_8: k' = 13.5, h_{min} = 2.03.

using reduced parameters and fitting the data via the van Deemter equation. The flow curves for the two phases and the van Deemter coefficients are shown in Fig. 11 and Table 3. The HC-C_8 (A = 1.05) is not quite as well-packed as the commercial sterically protected C_{18} phase (A = 0.88). This is not surprising because the packing procedure for the HC-C_8 was not optimized. The B term values for both phases are higher than theoretical but this is often observed [47,50]. Additional low ν data is needed to attain a more meaningful value for B. It is also evident that the resistance to mass transfer in the stationary zone is slightly higher for the HC-C_8 (C = 0.06) compared to the sterically protected C_{18} (C = 0.04). This result is also not very surprising because the HC-C_8 phase before it is acid aged has about 3% (w/w) more carbon than the sterically protected C_{18}. Despite the lack of packing and synthetic optimization, the HC-C_8 gives chromatographic efficiency which is quite acceptable for non-electrolyte solutes. The plate counts for a wide variety of non-electolyte solutes are given in Table 6. The average plate count is nearly 100,000/m and there are no systematic variations in N with retention factor. The only unusual result is the low efficiency observed for benzophenone.

Table 3
Comparison of van Deemter flow curve coefficients for sterically protected C_{18} and the HC-C_8 stationary phases[a,b,c]

Stationary phase	A	B	C
Sterically protected C_{18}	0.88 ± 0.03	8.22 ± 0.12	0.04 ± 0.005
HC-C_8	1.05 ± 0.04	4.06 ± 0.16	0.06 ± 0.007

[a] Solute = butanophenone.
[b] Mobile phase = 30/70 ACN/H_2O.
[c] T = 40 °C.

3.7. Retention characterization of the HC-C_8.

3.7.1. Linear solvent strength characterization

The linear relationship given below is often used to correlate the retention factor (k') of non-ionic solutes in RPLC with the volume fraction of organic modifier (ϕ) in the mobile phase.

$$\log k' = \log k'_W - S \cdot \phi \quad (2)$$

where, k'_w is the extrapolated retention of the solute in 100% water and S is a solute specific parameter that controls the change in k' for a given change in ϕ. It is important to remember that this relationship is only accurate (<1–2% deviation) over narrow ranges in ϕ ($\Delta\phi$ = 0.20–0.40). A representative plot of $\log k'$ versus ϕ for some alkylphenones on the HC-C_8 stationary phase is shown in Fig. 12.

The slopes and correlation coefficients obtained by linear regression of the data are summarized in Table 4. Overall, for non-ionic solutes the HC-C_8 phase behaves as a typical reversed phase material. The slopes (S) increase as the hydrophobicity of the solute increases in all three types of mobile phases. Additionally, the correlation coefficients are all above 0.995 indicating that the linear relationship given above adequately describes the retention data.

3.7.2. Analysis of retention energetics

The free energy of transfer per methylene unit is an important measure of phase hydrophobicity [51–54]. The magnitude of the free energy of transfer per methylene unit allows a direct quantitative comparison of the hydrophobicity of different stationary phases. It can be calculated from the Martin equation as follows:

$$\log k' = A + Bn_{CH_2} \quad (3)$$

Linear regression analysis of $\log k'$ versus n_{CH_2} allows the free energy of transfer per methylene unit to be calculated

Table 4
Summary of the statistical results of the linear solvent strength[a] regression for the HC-C_8 phase

	Intercept (±S.D.)			Slope (±S.D.)			R^2			S.E.[b]		
	ACN	CH_3OH	THF	CAN	CH_3OH	THF	ACN	CH_3OH	THF	ACN	CH_3OH	THF
Acetophenone	1.27 (±0.02)	1.98 (±0.01)	1.24 (±0.03)	2.40 (±0.04)	2.60 (±0.01)	2.76 (±0.07)	0.999	0.999	0.998	0.008	0.002	0.012
Butanophenone	2.08 (±0.05)	3.04 (±0.01)	2.15 (±0.05)	3.25 (±0.10)	3.53 (±0.01)	4.11 (±0.13)	0.998	0.999	0.997	0.019	0.002	0.021
Hexanophenone	2.91 (±0.09)	4.17 (±0.01)	3.09 (±0.09)	4.18 (±0.18)	4.52 (±0.02)	5.7 (±0.24)	0.996	0.999	0.995	0.035	0.003	0.038

[a] All chromatograms used for the study were obtained at T = 30 °C and F = 1.0 mL/min. The mobile phase composition for the ACN, methanol and THF runs ranged from 35–60%, 60–85% and 25–45%, respectively.
[b] Standard error of the fit.

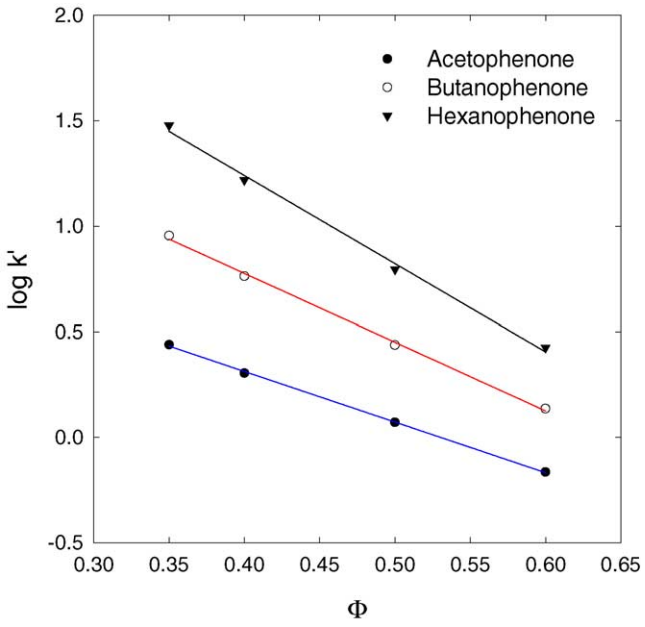

Fig. 12. Linear solvent strength characterization of HC-C_8 using ACN/H_2O mobile phases. T = 35 °C; flow rate = 1.0 mL/min.

from the slope, B from the equation:

$$\Delta G^{\circ}_{CH_2} = -2.3RTB \quad (4)$$

The $\log k'$ versus n_{CH_2} plots for four homologous series and the calculated $\Delta G^{\circ}_{CH_2}$ data for the HC-C_8 and some widely used stationary phases are given in Fig. 13 and Table 5, respectively. For all of the homologous series tested, the HC-C_8 phase is more retentive than a phenyl stationary phase. This result is not very surprising since the HC-C_8 phase has both phenyl and alkyl moieties in the stationary phase. The HC-C_8 stationary phase is less retentive than the highly aromatic PRP-1 (Hamilton) phase. Again, this is not surprising, as the PRP-1 phase is an entirely aromatic polymeric particle, it has a drastically higher density of phenyl rings across its surface than does the HC-C_8 phase, thus leading to a more favorable free energy of transfer per methylene unit.

To further compare the energetics of retention of the HC-C_8 stationary phase to several commonly used phases, plots of

Table 6
LSER descriptors[a] and average plate counts for the 22 non-electrolyte solutes

Solutes	V_2	π_2^*	$\sum\alpha_2^H$	$\sum\beta_2^H$	R_2	Plates/m
Benzene	0.7164	0.52	0	0.14	0.610	101,000
Toluene	0.8573	0.52	0	0.14	0.601	100,000
Ethylbenzene	0.9982	0.51	0	0.15	0.613	100,000
p-Xylene	0.9982	0.52	0	0.16	0.613	95,000
Propylbenzene	1.1391	0.50	0	0.15	0.604	90,000
Butylbenzene	1.280	0.51	0	0.15	0.600	85,000
Naphthalene	1.0854	0.92	0	0.20	1.340	93,000
p-Dichlorobenzene	0.9612	0.75	0	0.02	0.825	98,000
Bromobenzene	0.8914	0.73	0	0.09	0.882	92,000
Nitrobenzene	0.8906	1.11	0	0.28	0.871	100,000
p-Nitrotoluene	1.0315	1.11	0	0.28	0.870	110,000
Anisole	0.9160	0.75	0	0.29	0.708	90,000
Benzonitrile	0.8711	1.11	0	0.33	0.742	86,000
p-Nitrobenzyl chloride	1.1539	1.34	0	0.40	1.080	84,000
Methylbenzoate	1.0726	0.85	0	0.46	0.733	78,000
Acetophenone	1.0139	1.01	0	0.48	0.818	94,000
Benzophenone	1.4808	1.50	0	0.50	1.447	41,000
3-Phenylpropanol	1.1978	0.90	0.30	0.67	0.821	88,000
Benzyl alcohol	0.9160	0.87	0.33	0.56	0.803	84,000
N-Benzylformamide	1.1137	1.80	0.40	0.63	0.990	91,000
Phenol	0.7751	0.89	0.60	0.30	0.805	92,000
p-Chlorophenol	0.8975	1.08	0.67	0.20	0.915	41,000

Plate count calculated at half height on a 4.6 mm × 50 mm Hypercrosslinked C_8 column in 50/50 ACN/H_2O.
[a] All data taken from Zhao [63].

Table 5
Summary of free energy of transfer per methylene unit[a] for various stationary phases[b,c]

Stationary phase	$\Delta G^{\circ}_{CH_2}$ (cal mol^{-1})			
	Alkylbenzenes	Alkylphenones	Alkylacetates	Alkylanilines
PRP-1	−294 ± 4	−340 ± 18	−316 ± 3	−293 ± 1
Phenyl	−197 ± 1	−215 ± 7	−228 ± 3	−189 ± 1
C_{18}	−311 ± 4	−322 ± 7	−321 ± 6	−303 ± 3
HC-C_8	−229 ± 3	−247 ± 7	−251 ± 3	−220 ± 6

[a] Average $\Delta G^{\circ}_{CH_2} = -237$ cal mol^{-1}.
[b] Data for PRP-1, phenyl and C_{18} phases adapted from Zhao [63].
[c] Mobile phases = ACN/H_2O, T = 35 °C, F = 1.0 mL/min.

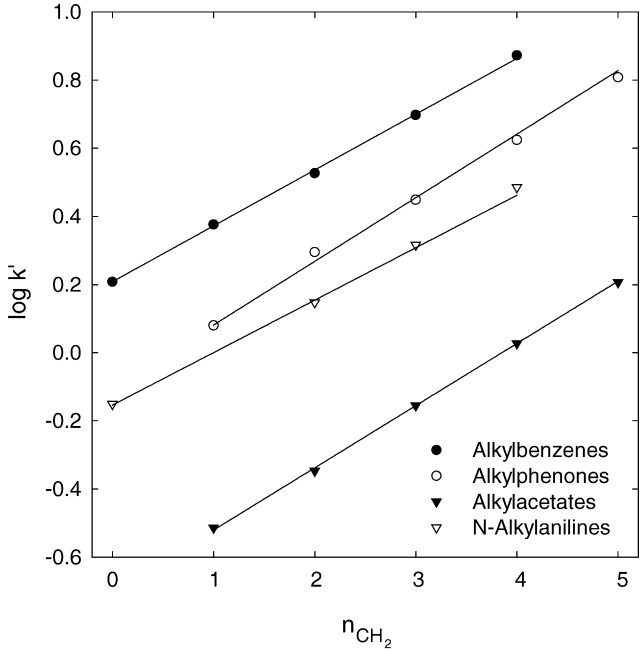

Fig. 13. Plot of log k' vs. n_{CH_2} for four homologous series on HC-C_8. Mobile phase: 50/50 ACN/H_2O; T = 35 °C; flow rate = 1.0 mL/min.

log k' (Phase X) versus log k' (HC-C_8) (κ–κ plots) for 22 non-ionic solutes with different molecular volume (V_2), dipolarity/polarizability (π_2^*), hydrogen bond donor acidity ($\sum \alpha_2^H$) hydrogen bond acceptor basicity ($\sum \beta_2^H$) and excess molar refraction (R_2) were generated. The 22 non-ionic solutes are listed in Table 6 along with their linear solvation energy relationship (LSER) descriptors and average plate counts on the HC-C_8 phase in 50/50 ACN/H_2O. This approach has been used by Horváth and coworkers [55], and Mao and Carr [56–59] to study the mechanism of retention and chromatographic selectivity. Horváth and coworkers [55] have stated that a good linear correlation with a slope of one indicates that the phases have identical energetics of retention. From a thermodynamic point of view they are homoenergetic. If the linear correlation is good, but the slope is not equal to one, then the thermodynamics of the retention processes on the two phases are similar (homeoenergetic). A poor linear correlation indicates significant differences in the intrinsic thermodynamic behavior (heteroenergetic) of the phases. This translates into major differences in chromatographic selectivity.

The κ–κ plots for a phenyl phase versus a Zorbax sterically protected C_8 phase and for phenyl phase versus the HC-C_8 phase are given in Fig. 14. The slope, good linear correlation and low standard deviation for the phenyl-Zorbax C_8 κ–κ plot indicates that the phases are homeoenergetic. Alternatively, the κ–κ plot for phenyl/HC-C_8 has a significantly lower correlation coefficient and a higher standard deviation. This indicates that the differences in selectivity between the HC-C_8 phase and the phenyl phase are larger than the differences between the phenyl phase and the Zorbax C_8. The

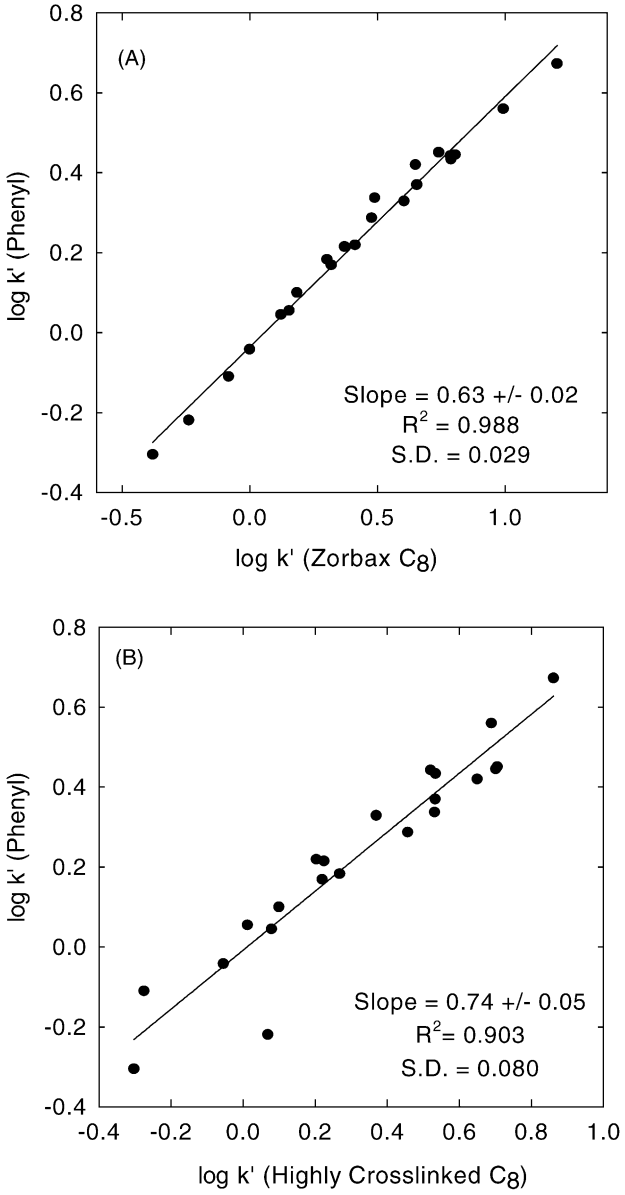

Fig. 14. κ–κ plot comparison of stationary phases using the LSER non-electrolyte solutes. Plot (A) phenyl vs. Zorbax C_8; plot (B) phenyl vs. HC-C_8; phenyl and Zorbax C_8 data adapted from Zhao [63]; T = 30 °C and F = 1.0 mL/min.

κ–κ plot comparison of Zorbax C_8 and PRP-1 versus HC-C_8 is given in Fig. 15. Again, the energetics of retention (i.e., selectivity) on the HC-C_8 are significantly different than the Zorbax C_8 and PRP-1 phases. Clearly, the HC-C_8 phase is an alkyl-aromatic phase that offers superb acid stability and has somewhat different chromatographic selectivity.

The differences in selectivity for non-electrolyte solutes for the HC-C_8, phenyl and C_8 phases are clearly shown in Fig. 16. By comparing the retention factors for the 22 solutes on all three columns in one plot, it is easy to see changes in retention order amongst the columns. It is clear that HC-C_8 phase offers selectivity that is different from both conventional C_8 and phenyl phases.

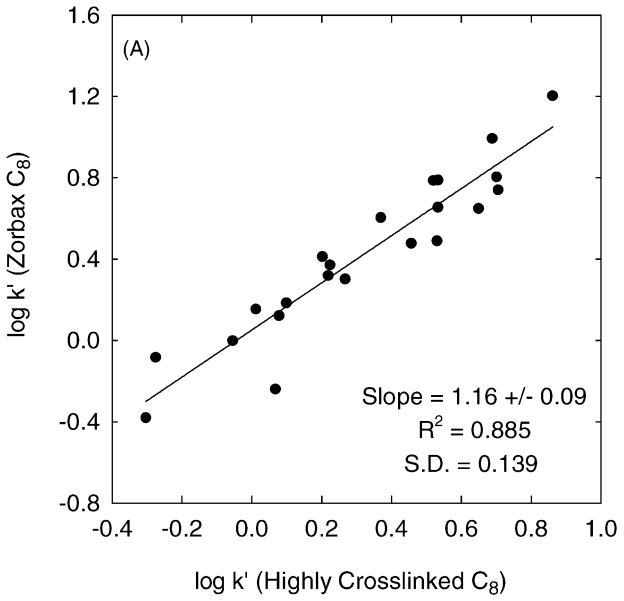

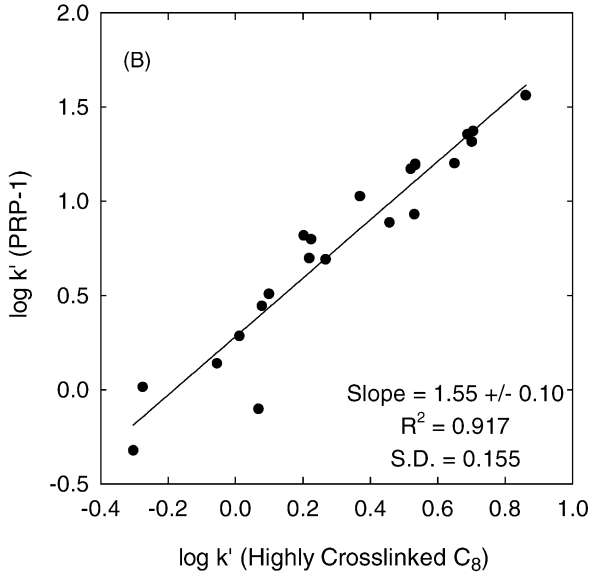

Fig. 15. κ–κ plot comparison of stationary phases using the LSER non-electrolyte solutes. Plot (A) Zorbax C_8 vs. HC-C_8; plot (B) Hamilton PRP-1 vs. HC-C_8; Zorbax C_8 and PRP-1 data adapted from Zhao [63]; T = 30 °C and F = 1.0 mL/min.

3.7.3. Characterization of shape and electron acceptor solute selectivity

Further selectivity characterization was performed using positional isomers and electron acceptor solutes. It is very important to probe the retention characteristics of the HC-C_8 phase with these types of solutes. For example, positional isomers are better separated on phases with conformationally more rigid surface such as PRP-1 and C_{30} bonded phase [60–62]. Additionally, electron acceptor solutes are useful for comparing the electron donor/acceptor capability of the stationary phases.

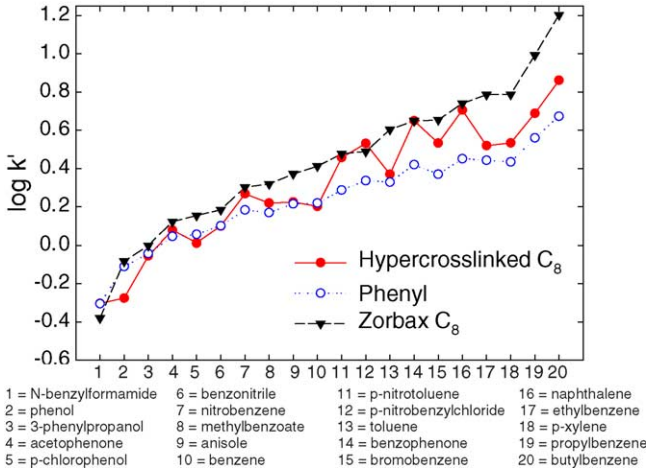

Fig. 16. Plot of log k' trends for LSER non-electrolyte solutes on three stationary phases.

The selectivity data for the positional isomers is summarized in Table 7. The HC-C_8 phase shows higher shape selectivity compared to the phenyl or C_{18} phases. It is possible that the HC-styrene heptamer on the silica is conformationally more rigid, thus it is better able to differentially retain these isomers. The shape selectivity of the HC-C_8 phase is better for some solute pairs and worse for others compared to the PRP-1 phase. PRP-1 is thought to retain solutes by a more adsorption-like mechanism, thus allowing for differentiation between positional isomers. Like all RPLC stationary phases, the exact details of the retention mechanism on the HC-C_8 are not well understood, but it is reasonable to conclude that this phase provides some unique shape selectivities.

The electron acceptor solute selectivities, $\alpha_{solute/benzene}$ for the HC-C_8 and two commonly used RPLC stationary phases are given in Table 8. With the exception of *p*-chlorophenol, the HC-C_8 phases offers the highest selectivity for the electron acceptor solutes. Based upon the definition of $\alpha_{solute/benzene}$, it is clear that the relative retention of electron acceptor solutes is significantly higher on the HC-C_8 stationary phase compared to the other phases. The HC-C_8 is phase is a better electron donor than even the phenyl stationary phase. The reason for this difference is not well understood at this time.

Table 7
Summary of selectivity factors for isomeric solutes on various stationary phases[a,b]

Stationary phase	Phenyltoluenes		Terphenyls	
	meta/ortho	para/meta	meta/ortho	para/meta
PRP-1	1.26	1.00	2.13	1.09
Phenyl SiO_2	1.03	1.00	1.13	1.07
C_{18} SiO_2	1.05	1.00	1.23	1.09
HC-C_8 SiO_2	1.18	1.08	1.67	1.35

[a] Data for Hamilton PRP-1, phenyl and C_{18} phases adapted from Zhao [63].
[b] Mobile phases = ACN/H_2O, T = 35 °C, F = 1.0 mL/min.

Table 8
Summary of selectivity factors for electron acceptor solutes on various stationary phases[a,b]

Solutes	$\alpha_{solute/benzene}$		
	Sterically protected C_{18}	Phenyl	HC-C_8
Nitrobenzene	0.73	0.92	1.24
p-Nitrotoluene	1.15	1.17	1.98
p-Nitrobenzyl chloride	1.16	1.31	2.40
Bromobenzene	1.88	1.42	2.38
p-Chlorophenol	0.45	0.69	0.66

[a] Data for PRP-1, phenyl and C_{18} phases adapted from Zhao [63].
[b] Mobile phases = ACN/H_2O, T = 35 °C, F = 1.0 mL/min.

4. Conclusions

Despite a tremendous improvement in acid stability, the highly crosslinked CMPES-SAM stationary phases as made here were not chromatographically useful. The SAM phase is substantially more silanophilic than is a sterically protected ODS stationary phases. ^{29}Si magic angle spinning cross-polarization solid-state NMR spectroscopy and peak shape comparisons indicate that the CMPES-SAM itself is the source of the silanophilicity. The SAM process and not the Friedel-Crafts crosslinking step is the cause of the poor peak shape and increased retention for basic solutes.

The obvious alternative to self-assembly of the chloromethylphenylethylsilane is monomeric silanization using dimethyl-chloromethyl-phenylethylsilane. This method of silanization is superior to self-assembly because additional silanol groups are not formed. By adjusting the Friedel-Crafts crosslinking conditions, a highly crosslinked styrene heptamer DM-CMPES has been developed. Despite the fact that the surface density of silane groups on the DM-CMPES phase is approximately 50% lower than that of the CMPES-SAM phase, a highly acid stable phase is formed by Friedel-Crafts crosslinking with styrene heptamer. The HC-styrene heptamer DM-CMPES and HC-C_8 phases provide better acid stability than the sterically protected ODS phase. The loss in k' of the new phase in hot acid is due, not to loss in amount of bonded material, but rather to slow changes in the chemistry of the bonded layer.

HC-C_8 gives quite acceptable peak shapes and retention factors for non-electrolyte solutes; however, the plate counts for basic solutes are lower than those obtained on the sterically protected C_{18} phase. A more detailed study of the factors influencing the silanophilicity and overload characteristics of this phase is currently underway. Inverse size exclusion chromatography and HETP/flow studies show no pore blockage and acceptable packing and mass transfer. The calculated free energy of transfer per methylene unit indicates that the HC-C_8 is less hydrophobic than a conventional C_{18} phase, but more hydrophobic than a conventional phenyl phase. Additionally, the HC-C_8 phase offers unique selectivity for positional isomers, electron acceptor solutes and the wide range of non-electrolyte solutes evaluated. Finally the plate counts of the 5 μm particles are typically 80,000–100,00/m for a wide variety of non-electrolytes.

References

[1] B.C. Trammell, L. Ma, H. Luo, D. Jin, M.A. Hillmyer, P.W. Carr, Anal. Chem. 74 (2002) 4634.
[2] C. McNeff, L. Zigan, K. Johnson, P. Carr, A. Wang, A. Weber-Main, LCGC 18 (2000) 514.
[3] P.W. Carr, High Stability Porous Zirconium Oxide Spherules, Regents of the University of Minnesota, 1991.
[4] P.W. Carr, Chromatography in Biotechnology, ACS Symposium Series No. 529, 1993, p. 146.
[5] P.W. Carr, J.A. Blackwell, P. Weber, W.A. Schafer, M.P. Rigney, Zirconium Oxide Based Supports for Biochromatographic Applications, ACS Symposium Series, 1993, p. 146.
[6] J.L. Glajch, J.J. Kirkland, Substrates with sterically protected, stable, covalently bonded organosilane films, U.S. Patent # 4,705,725 (1987).
[7] J.L. Glajch, J.J. Kirkland, Structures surface modified with bidentate silanes, U.S. Patent # 4,746,572 (1988).
[8] J.L. Glajch, J.J. Kirkland, Substrates coated with organosilanes that are sterically protected, U.S. Patent # 4,847,159 (1989).
[9] J.J. Kirkland, J.L. Glajch, R.D. Farlee, Anal. Chem. 61 (1989) 2.
[10] J.J. Kirkland, J.B. Adams, M.A.V. Straten, H.A. Claessens, Anal. Chem. 70 (1998) 4344.
[11] J.J. Kirkland, J.B. Adams, Asymmetric bidentate silanes, U.S. Patent # 5,869,724 (1999).
[12] J. Nawrocki, C.J. Dunlap, P.W. Carr, J.A. Blackwell, Biotechnol. Prog. 10 (1994) 561.
[13] J. Nawrocki, M.P. Rigney, A. McCormick, P.W. Carr, J. Chromatogr. A 657 (1993) 229.
[14] U.D. Neue, R.A. Meyers, Encyclopedia of Analytical Chemistry, John Wiley and Sons, New York, 2001.
[15] M.P. Rigney, The Development of Porous Zirconia as a Support for Reversed-phase High Performance Liquid Chromatography, University of Minnesota, Minneapolis, Minnesota, 1989.
[16] M.P. Rigney, T.P. Weber, P.W. Carr, J. Chromatogr. 484 (1989) 273.
[17] M.J. Wirth, R.W.P. Fairbank, H.O. Fatunmbi, Science 275 (1997) 44.
[18] M.J. Wirth, H.O. Fatunmbi, Products having multiple substituted polysiloxane monolayer, U.S. Patent # 5,599,625 (1997).
[19] M.J. Wirth, H.O. Fatunmbi, Products having multiple substituted polysiloxane monolayer, U.S. Patent # 5,716,705 (1998).
[20] L. Sun, Polybutadiene-Coated Zirconia as a Biocompatible Reversed-Phase High Performance Liquid Chromatography Support Chemistry, University of Minnesota, Minneapolis, 1994.
[21] L. Sun, P.W. Carr, Anal. Chem. 67 (1995) 3717.
[22] B.C. Trammell, L. Ma, H. Luo, M.A. Hillmyer, P.W. Carr, J. Am. Chem. Soc. 125 (2003) 10504.
[23] J.D. Thompson, P.W. Carr, Anal. Chem. 73 (2001) 3340.
[24] J.D. Thompson, P.W. Carr, Anal. Chem. 74 (2002) 4150.
[25] J.D. Thompson, P.W. Carr, Anal. Chem. 74 (2002) 1017.
[26] B. Yan, J. Zhao, J. Brown, J. Blackwell, P. Carr, Anal. Chem. 72 (2000) 1253.
[27] D.H. Reeder, J.W. Li, P.W. Carr, M.C. Flickinger, A.V. McCormick, J. Chromatogr. A 760 (1997) 71.
[28] J.W. Li, D.H. Reeder, A.V. McCormick, P.W. Carr, J. Chromatogr. A 791 (1998) 45.
[29] M. Hanson, B. Eray, K. Unger, A.V. Neimark, J. Schmid, K. Albert, E. Bayer, Chromatographia 35 (1993) 403.
[30] M.P. Tsyurupa, T.A. Mrachkovskaya, L.A. Maslova, G.I. Timofeeva, L.V. Dubrovina, E.F. Titova, V.A. Davankov, V.M. Menshov, React. Polym. 19 (1993) 55.

[31] V.A. Davankov, M.M. Ilyin, M.P. Tsyurupa, G.I. Timofeeva, L.V. Dubrovina, Macromolecules 29 (1996) 8398.
[32] V.A. Davankov, M.P. Tsyurupa, React. Polym. 13 (1990) 27.
[33] R.W.P. Fairbank, Y. Xiang, M.J. Wirth, Anal. Chem. 67 (1995) 3879.
[34] J.G. Dorsey, Ultrasound driven synthesis of reversed and normal phase stationary phases for liquid chromatography, U.S. Patent # 4,919,804 (1990).
[35] I. Halasz, K. Martin, Ber. Busenges Phys. Chem 79 (1975) 731.
[36] I. Halasz, K. Martin, Angew. Chem. 90 (1978) 954.
[37] J.W. Li, P.W. Carr, Anal. Chem. 69 (1997) 2550.
[38] H.O. Fatunmbi, M.D. Bruch, M.J. Wirth, Anal. Chem. 65 (1993) 2048.
[39] M. Wirth, Personal Communication, HPLC 2004, Chicago, IL, 2004.
[40] H. Engelhardt, G. Ahr, Chromatographia (1981) 14.
[41] L.R. Snyder, J.L. Glajch, J.J. Kirkland, Practical HPLC Method Development, Wiley-Interscience, New York, 1996.
[42] D.V. McCalley, Anal. Chem. 75 (2003) 3072.
[43] C.J. Dunlap, P.W. Carr, A.V. McCormick, Chromatographia 42 (1996).
[44] B. Gawdzik, J. Osypiuk, Chromatographia 54 (2001) 595.
[45] D.H. Reeder, A.M. Clausen, M.J. Annen, P.W. Carr, M.C. Flickinger, A.V. McCormick, J. Colloid Interface Sci. 184 (1996) 328.
[46] J.W. Li, P.W. Carr, Anal. Chem. 69 (1997) 2193.
[47] J.H. Knox, H. Scott, J. Chromatogr. 282 (1983) 297.
[48] K.K. Unger, Packings and Stationary Phases in Chromatographic Techniques, M. Dekker, New York, 1989.
[49] K.K. Unger, J. Chromatogr. 660 (1994) 97.
[50] R.W. Stout, J.J. DeStefano, L.R. Snyder, J. Chromatogr. 282 (1983) 263.
[51] J.H. Park, Y.K. Lee, Y.C. Weon, J.W. Li, L. Li, J.F. Evans, J. Chromatogr. A 767 (1997) 1.
[52] P.W. Carr, J.J. Li, A.J. Dallas, D.I. Eikens, L.C. Tan, J. Chromatogr. A 656 (1993) 113.
[53] P.W. Carr, L.C. Tan, J.H. Park, J. Chromatogr. A 724 (1996) 1.
[54] L.C. Tan, P.W. Carr, J. Chromatogr. A 775 (1997) 1.
[55] W. Melander, J. Stoveken, Cs. Horváth, J. Chromatogr. 199 (1980) 35.
[56] Y. Mao, P.W. Carr, Anal. Chem. 72 (2000) 2788.
[57] Y. Mao, P.W. Carr, Anal. Chem. 72 (2000) 110.
[58] Y. Mao, P.W. Carr, Anal. Chem. 73 (2001) 4478.
[59] Y. Mao, P.W. Carr, Anal. Chem. 2001 (2001) 1821.
[60] L.C. Sander, S.A. Wise, Anal. Chem. 56 (1984) 504.
[61] L.C. Sander, S.A. Wise, Anal. Chem. 59 (1987) 2309.
[62] L.C. Sander, S.A. Wise, J. Chromatogr. 656 (1993) 335.
[63] J. Zhao, P.W. Carr, Anal. Chem. 70 (1998) 3619.